



HAL
open science

Interference thresholds for active implantable cardiovascular devices in occupational low-frequency electric and magnetic fields: a numerical and in vitro study

Mengxi Zhou, Djilali Kourtiche, Julien Claudel, Francois Deschamps, Isabelle Magne, Patrice Roth, Pierre Schmitt, Martine Souques, Mustapha Nadi

► To cite this version:

Mengxi Zhou, Djilali Kourtiche, Julien Claudel, Francois Deschamps, Isabelle Magne, et al.. Interference thresholds for active implantable cardiovascular devices in occupational low-frequency electric and magnetic fields: a numerical and in vitro study. *Medical Engineering & Physics*, 2022, 104, pp.103799. 10.1016/j.medengphy.2022.103799 . hal-03919083

HAL Id: hal-03919083

<https://hal.univ-lorraine.fr/hal-03919083>

Submitted on 22 Jul 2024

HAL is a multi-disciplinary open access archive for the deposit and dissemination of scientific research documents, whether they are published or not. The documents may come from teaching and research institutions in France or abroad, or from public or private research centers.

L'archive ouverte pluridisciplinaire **HAL**, est destinée au dépôt et à la diffusion de documents scientifiques de niveau recherche, publiés ou non, émanant des établissements d'enseignement et de recherche français ou étrangers, des laboratoires publics ou privés.



Distributed under a Creative Commons Attribution - NonCommercial 4.0 International License

1 **Title**

2 Interference thresholds for active implantable cardiovascular devices in occupational low-frequency
3 electric and magnetic fields: a numerical and in vitro study

4 **Author names and affiliations**

5 Mengxi Zhou^a, Djilali Kourtiche^a, Julien Claudel^a, Francois Deschamps^b, Isabelle Magne^c, Patrice Roth^a,
6 Pierre Schmitt^a, Martine Souques^c, Mustapha Nadi^a

7 ^a Université de Lorraine, Institut Jean Lamour (UMR 7198), CNRS, 2 allée André Guinier, Campus
8 Artem, 54000 Nancy , France

9 ^b RTE, Direction Développement Ingénierie, Département Concertation et Environnement, Place du
10 Dôme 92073 Paris La Défense Cedex

11 ^c EDF , Service des Etudes Médicales, Immeuble Smartside, Bâtiment Bréchet, 4ème étage, zone 4-680
12 4 rue Floréal, 75017 Paris

13 **Corresponding author**

14 Mengxi ZHOU

15 Email: mengxi.zhou@univ-lorraine.fr

16 Institut Jean Lamour (UMR 7198), CNRS, 2 allée André Guinier, Campus Artem, 54000 Nancy ,
17 France

18 **Abstract**

19 In light of concerns regarding the occupational safety and health of workers wearing active implantable
20 medical devices (AIMDs), this study aims to investigate the potential risks of electromagnetic
21 interference (EMI) between AIMDs and low-frequency 50/60 Hz electromagnetic fields (EMFs) in the
22 workplace.

23 A total of 58 AIMDs, consisting of pacemakers (PMs) and implantable cardiac defibrillators (ICDs) of
24 different brands, models, and configurations were tested to determine the immunity thresholds for high-
25 voltage electric fields (EFs) and magnetic fields (MFs) at 50/60 Hz. The EFs and MFs at the levels in
26 workplaces are reproduced by setups using Helmholtz coils and aluminum plates, respectively, to ensure
27 that the EM/MF exposures are controllable and reproducible. The EMI thresholds were recorded by
28 observing the occurrences of PM or ICD dysfunctions. In addition, numerical studies on anatomical
29 models were carried out using CST[®] software.

30 The results indicate that the recorded thresholds all exceed the EF and MF public exposure limits given
31 in the ICNIRP 2010 guidelines. No dysfunction was observed among four ICDs tested under MF
32 exposure up to 2750 μ T at 50 Hz and 2480 μ T at 60 Hz. However, among the 43 PMs and 11 ICDs
33 tested under EF exposures, potential hazards may occur below the occupational exposure level proposed
34 in the ICNIRP guidelines.

35 **Keywords:** Electromagnetic Interference (EMI), Active Implantable Medical Device (AIMD),
36 Occupational exposure, Immunity thresholds, 50/60 Hz

37 Introduction

38 Active implantable medical devices (AIMDs) are extensively used in the treatment and diagnosis of
39 various diseases. Cardiovascular disease is the leading cause of death in the United States, responsible
40 for approximately 659,000 deaths per year, accounting for 25% of all deaths^[1]. In Europe, it causes 3.8
41 million deaths each year, accounting for 45% of all deaths^[2]. Approximately 500,000 pacemaker (PM)
42 implantations were performed in 2016, and 100,000 cardioverter defibrillators (ICDs)^[3] were implanted
43 in Europe. On the other hand, with the continuous upgrading of global electrification and wireless
44 technologies, humans are confronting unprecedented and inevitable EMFs in their surroundings. From
45 medical radiography using X-ray to every power socket associated with low-frequency EMFs, EMF
46 sources play an important role in human daily life. Thus, the fact of AIMD carriers submitted to
47 electromagnetic fields (EMFs) is a subject of great concern. This is especially the case for patients
48 bearing cardiac implants.

49 The risks to AIMDs in the presence of strong EMFs must be assessed. They cannot be neglected,
50 considering that cardiac implants are vital and life-saving devices. Numerous studies have been carried
51 out aiming to test AIMDs in electric fields (EFs) or magnetic fields (MFs) in different frequency ranges
52 and by different approaches. *In vitro* tests for the risk assessment were conducted in Italy for workers
53 with AIMDs exposed to different EMF sources: an electrosurgical unit, transcranial magnetic
54 stimulation, and an arc welder^[4]. PMs and ICDs were studied in Finland using a human-shaped phantom
55 exposed to EMFs under a 400kV power line and at 220kV/400kV substations^{[5][6][7]}. Other *in vivo* studies
56 investigated the occurrence of electromagnetic interference with PMs caused by common environmental
57 sources of EMFs: mobile phone base stations, electrically powered commuter trains, overhead high-
58 voltage transmission lines, and magnetic resonance imaging^{[8][9][10]}.

59 Exposures to high-power EMFs (50/60 Hz) are commonly found in the electrical supply industry, where
60 workers may be exposed to MFs, which can exceed 1000 μ T, and to EFs, which can exceed 10 kV/m.
61 For such occupational environments, the risk of malfunction and that of other safety threats to cardiac
62 implant wearers need to be investigated. Thus, a system of validation needs to be set up which allows
63 employers to verify whether workers can return to their posts after having cardiac AIMDs implanted.
64 The EMF limit values are defined as a basic restriction in ICNIRP 2010 guidelines^[11], to prevent the
65 possibility of adverse health effects caused by external EFs and MFs. According to ICNIRP guidelines,
66 reference levels for general public exposure are defined as 5 kV/m for EFs and 200 μ T for MFs at 50
67 Hz; 4.17 kV/m for EFs and 200 μ T for MFs at 60 Hz. For occupational exposure, the reference levels
68 are defined as 10 kV/m for EFs and 1000 μ T for MFs at 50 Hz; 8.33 kV/m for EFs and 1000 μ T for
69 MFs at 60 Hz. Risk assessment of active implantable devices in professional low-frequency EMF
70 environments is proposed in the European standard series EN 50527^[12]. They provide the procedures
71 for evaluating the risks of EMF exposures to a worker bearing a cardiac implant (PM or ICD) in the
72 occupational environment.

73 Since 2005, our team has developed different studies to evaluate the immunity of PMs and ICDs under
74 low frequency (mainly 50/60 Hz) EMF exposure. These studies were conducted both theoretically as
75 well as experimentally, *in vitro*. Our main goal was to establish a risk assessment for cardiac implant
76 wearers under occupational exposures. In previous investigations, we performed numerical studies and
77 *in vitro* studies which allowed more controllable experimental conditions, such as frequency ranges,
78 system configurations, sensitivity levels of implanted devices, and more. We conducted *in vitro* studies
79 on the immunity of cardiac implants exposed to MFs^[13] and EFs^[14], respectively. The studies involved
80 PMs and ICDs. An *in vitro* cost-effective test bench was proposed in order to reproduce induced
81 phenomena on a cardiac implant inside a human body exposed to EFs^[15]. A phantom respecting the
82 induction occurring inside the human body was used in the *in vitro* experiments, referring to the
83 induction level simulated on an anatomical human body model. Interference with PMs for various lead

84 configurations and implantation positions were also computed on the anatomical model exposed to a
85 50Hz EF, using CST EM[®] 3D software^[16].

86 In this paper, we have summarized the methods applied and the results obtained by our group for MF
87 and EF exposure. They are discussed in the frame of the risk assessments proposed by the standard EN
88 50527.

89

90 **Methods**

91 According to Faraday's law of induction, a time-varying MF induces an electric current in the conductor.
92 For a human body exposed to an MF, internal currents may be induced in the body's tissues. EN 62226-
93 2-1 proposed different methods for calculating this induced EF in simple 2D models under MF
94 exposures^[17]. For a single frequency, assuming the body, or the part of the body exposed, is a circular
95 section of radius r , with conductivity σ , the induced current density can be calculated by reference to the
96 external magnetic flux density, as follows:

$$97 \quad J_{in} = \sigma \pi r f B_{ex} \quad [1],$$

98 where J_{in} is the current density induced at the circle of radius r , f is the frequency, and B_{ex} is the external
99 magnetic flux density. The value of induced currents is minimum at the center and maximum at the edge.

100 Alternating EFs cause displacement of electric charges in conductive media, resulting in an "induced"
101 alternating current inside it. For a human body exposed to an EF, the induced current may occur in the
102 body. EN 62226-3-1^[18] proposed methods for calculating the internal induced current under low-
103 frequency EF exposures. The relation between the external field and the internal induced current density
104 can be determined using a shape factor, as follows:

$$105 \quad J_{in} = k \times f \times E_{ex} \quad [2],$$

106 where J_{in} is the current density induced within the conductive material, f is the frequency, E_{ex} is the
107 vertical external EF, and k is the shape factor, which depends on the geometry. In other words, for a
108 human body exposed to an EF at a certain frequency, the induced current depends on its geometry, the
109 ratio of length to the radius (L/R) of the body, and the location within the body where J_{in} is calculated.

110 From the value of the induced current density J_{in} , the internal electric field E_i can be easily derived
111 according to Ohm's law:

$$112 \quad J_{in} = \sigma \times E_i \quad [3],$$

113 where J_{in} is the current density induced, σ is the conductivity, and E_i is the internal electric field. In other
114 words, the internal electric fields are induced in the body tissues when exposed to an EF or an MF. For
115 an AIMD wearer exposed to an EF or an MF, the internal EF will be induced as well as on the device
116 input, which may be disturbed by the EM interference. The investigation of the susceptibility of AIMDs
117 was based on the estimation of the induced voltage on the device input.

118 A cardiac implant (PM or ICD) consists of an impulse generator embedded in a closed metallic box and
119 a lead with two possible configurations: unipolar or bipolar. In unipolar sensing mode, the cardiac signal
120 is sensed between the metallic container and an electrode at the end of the lead; in bipolar sensing mode,
121 the cardiac implant senses the signal between two electrodes (tip and ring) at the respective extremities
122 of the lead. The evaluation of the induced voltage on the cardiac implant can be obtained by integration
123 according to the following classical equation^[22]:

$$124 \quad U = \int_{Tip}^{Generator / Ring} \vec{E} \cdot d\vec{l} \quad [4].$$

125

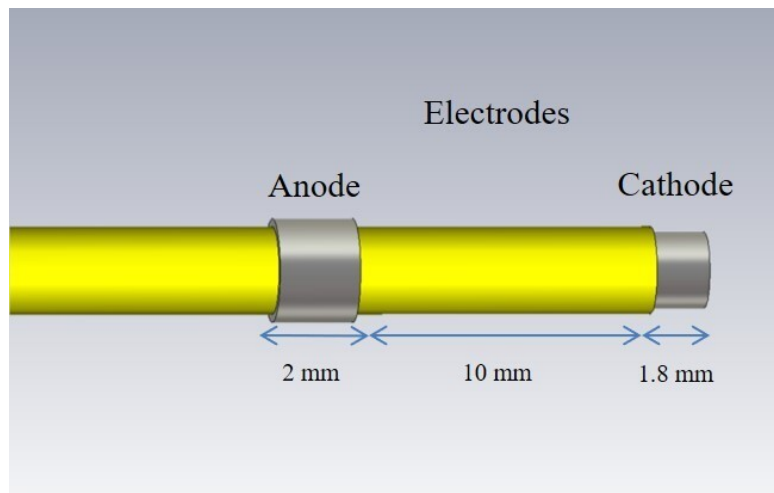
126 In this study, theoretical modeling of the behavior of PMs and ICDs exposed to EMFs was carried out
127 in parallel with experimental studies. CST EM[®] software, based on the finite integration technique, was
128 used for the simulations with the electro/magneto-quasi-static equations. We limited the frequency band
129 of the occupational exposures to the low frequency EM fields (50/60 Hz); thus the studies of exposures
130 to the EFs and MFs were carried out separately.

131

132 1. Numerical approach

133 ● Cardiac Implant Model

134 The model of a cardiac implant is composed of a metallic box representing the impulse generator
135 (Dimensions: 3 cm×4 cm for PM, 4 cm×6 cm for ICD) and a bipolar lead with electrodes at the tip
136 (Figure 1). In the numerical modeling, the container of the impulse generator is made of titanium (σ :
137 2.38×10^6 S/m) and the lead electrodes are made of platinum (σ : 9.52×10^6 S/m). The insulator of the lead
138 has a conductivity of 10^{-12} S/m and a permittivity of 6. This model of cardiac implant remains the same
139 for EF exposure and MF exposure.



140

141 **Figure 1.** Structure and Dimensions of a Bipolar Probe of the Cardiac Implant (the Lead Electrodes in
142 Gray and the Insulator in Yellow)

143

144 ● Anatomical Model

145 M Numerical

146 An anatomical human body model, derived from high resolution magnetic resonance images of healthy
147 volunteers^[19], was used in the numerical simulation of MFs. The model represents a 34-year-old male
148 of 1.77 m and 76 kg, based on a realistic external shape composed of 5 mm cubic voxels. Each voxel is
149 characterized by the conductivity corresponding to the associated tissue from calculations based on the
150 algorithms provided in Camelia Gabriel's (1996) report. The anatomical model implanted with a cardiac
151 device was placed in a homogeneous MF. A systematic study on the induced voltage calculation between
152 the distal and proximal electrodes was carried out in terms of the source position and frequency.

153 E Numerical

154 In the study of EF exposures, a 2 mm resolution surface-based model (Ansoft, Ansys[®]) was used,
155 presenting an anatomical male of 183.6 cm tall in standing position, with arms closed on the side and

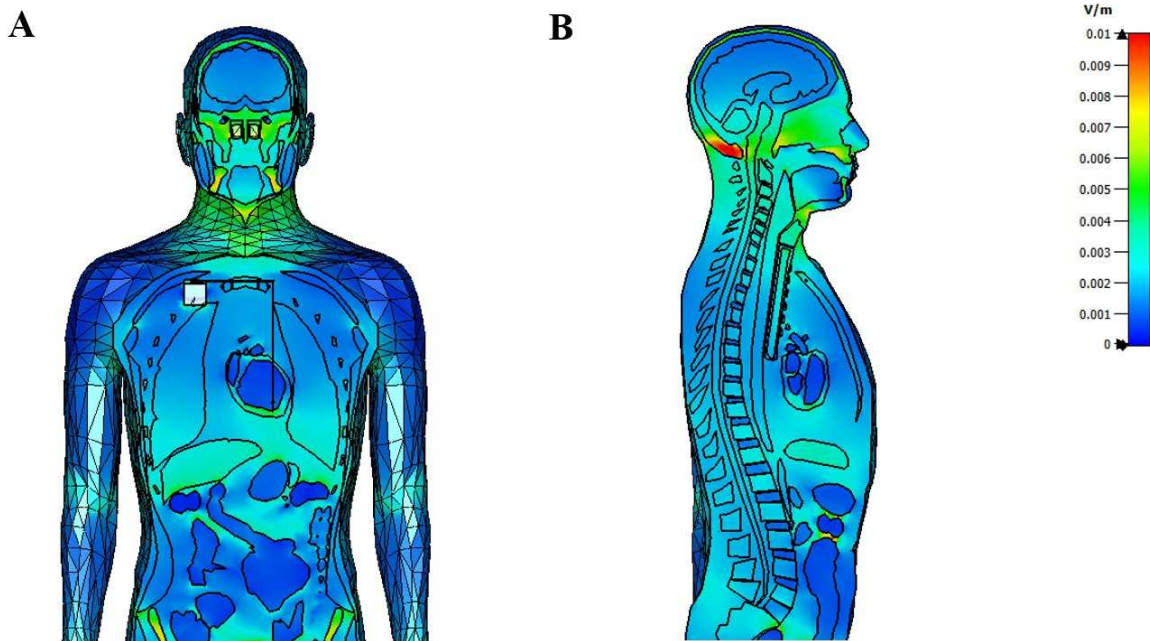
156 grounded feet. The model, constructed with 272 organs and 32 tissues with the dielectric properties of
 157 the IT'IS database^[20], was simulated under 1 kV/m 50 Hz EF exposure. Compared to the voxel model
 158 using hexahedral mesh, the tetrahedral mesh of Ansoft model respects the rounded geometries of organs
 159 and avoids the step effect. The induced EFs on the organs are given in Table 1.

160 **Table 1.** Ansoft body model (2 mm resolution) exposed to a 50 Hz uniform EF, maximum induced EF
 161 on the organs (mV/m) per 1 kV/m

Organ Name	Isotropic $\sigma^{[20]}$	E_{avg}	E_{max}
Unit	S/m	$mV \cdot m^{-1}$	$mV \cdot m^{-1}$
Brain	0.08	0.9	1.7
Heart muscle	0.08	1.14	4
Heart lumen	0.70	0.545	2.44
Muscle	0.35	1.25	29.4
Skin	0.10	1.43	77.3

162

163 The cardiac implant model was implanted in the 2 mm resolution Ansoft anatomical model under 1
 164 kV/m 50 Hz exposure for numerical computations. The induced voltage on the cardiac implant can be
 165 affected by several factors. We performed studies on the influence of the sensing mode, the lead
 166 dimensions, the tip position, the chamber impact, and the sensitivity settings of the cardiac implant^[16].



167

168 **Figure 2.** Induced EFs on the 2 mm resolution Ansoft anatomical model with a cardiac implant under
 169 1 kV/m 50 Hz exposure (A) Front view; (B) Side view.

- 170 ● Exposure system

171 M Numerical

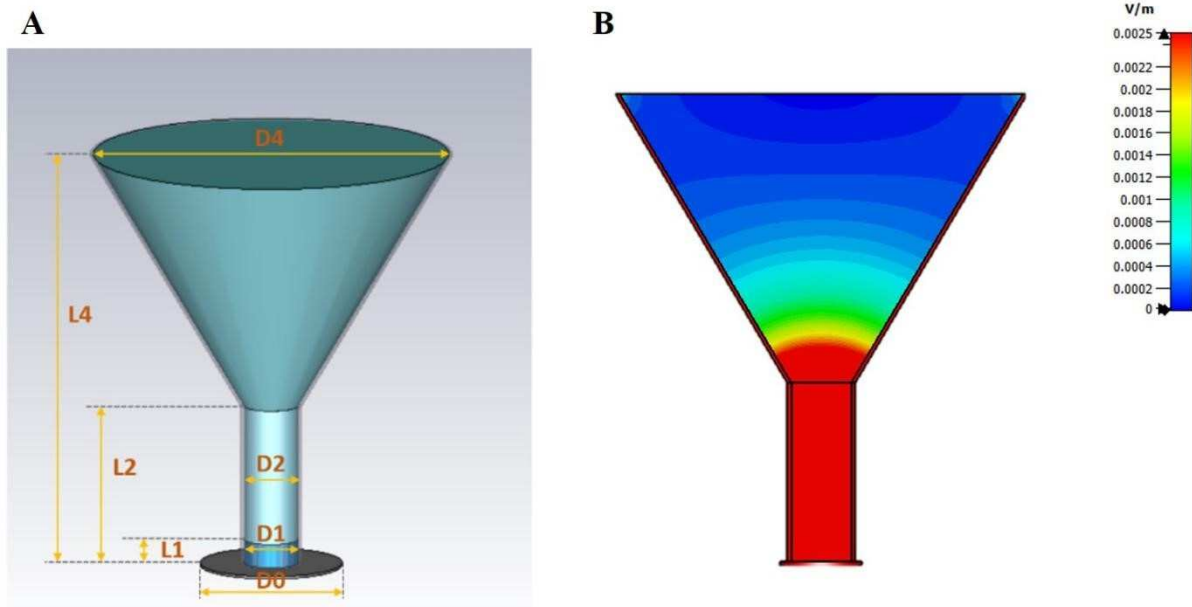
172 Numerical studies of the experimental exposure systems were conducted as well. The Helmholtz coil is
 173 most commonly used for low frequency MF sources, due to the homogeneity it provides. To ensure that
 174 the experimental model was entirely exposed in the homogeneous MF, we used two coils with radii of

175 520 mm, 520 mm apart. This is the MF exposure source we chose for both the modeling and the
176 experimental approaches. A phantom tank (Height: 15 cm; Width: 30 cm) filled with gelatin, to simulate
177 the electrical properties of biological tissues based on the study of Marchal et al.^[21], was used in the
178 experiments. The phantom tank was modeled as a homogeneous brick filled with a 0.1 S/m solution in
179 the numerical simulation, close to the conductivity of heart muscle in the voxel model 0.087 S/m^[19]. A
180 bipolar ICD model was inserted into the brick. The distance between the two bipolar electrodes (tip to
181 ring) was set to the typical distance of 10 mm. The tip-to-ring pair was placed in perpendicular to an
182 imaginary line from the impulse generator and the tip-to-ring pair, in order to reach to the maximum
183 induction area.

184 **E Numerical**

185 In the study of EF exposure, a homogeneous EF was generated between two parallel square plate
186 conductors (aluminum σ : 3.56×10^7 S/m), each with a side length of 2 m, separated by a distance of 0.75
187 m. A potential V was applied on one plate; the other plate was grounded. The porcelain insulators (ϵ : 6;
188 σ : 10^{-15} S/m) as supports between the plates were also investigated. We barely detected any influence of
189 the insulators on the EF, except in a zone close to them (r : 5 cm). The dimensions and construction of
190 the exposure system are preserved in the experimental approach.

191 Rectangular phantoms and human-shape phantoms are commonly used in *in vitro* experiments
192 simulating body tissues. Due to the complexity of the human body, these phantoms cannot present the
193 shape influence of the human body or the induction diversity of different tissues for EF exposure.
194 According to the numerical analysis of the Ansoft anatomical model, under 1 kV/m 50 Hz electric field
195 exposure, the maximum induced EF in the heart is 4 mV/m, and the mean induced EF over the thorax
196 is 0.8 mV/m. In the study of EF exposures, we used a phantom that reproduces the environment where
197 the PM or ICD is implanted. The phantom was reduced to 1/5 height (L4: 0.352 m) of the human
198 reference. To maintain the shape factor k, which depends on the ratio L/R, the circumference was
199 deduced accordingly. The phantom is made of 3.3 mm glass filled with a 0.2 S/m solution, composed
200 of a cylinder part and a cone part. Under 1 kV/m 50 Hz electric field exposure, constant EF induction
201 (4 mV/m) occurs in the cylinder part (D2: 0.046 m, L2: 0.135 m), representing the maximum induction
202 over the heart where the probe is placed in the human body. The probe was always placed parallel to the
203 external EF, in order to reach the maximum induction. The cone part (D4: 0.3 m) represents the mean
204 level of induction over the thorax (0.8 mV/m), which contains the generator (Figure 3). A metallic
205 pedestal (D1: 0.046 m, D0: 0.12 m) is plugged into the bottom of the container to keep the phantom in
206 the vertical position and grounded. L3 and D3 represent the height and the diameter, respectively, of the
207 filled solution. In this case, the phantom is fulfilled (L3: 0.352 m, D3: 0.3 m).



208

209

210

Figure 3. Experimental phantom. (A) Dimensions of phantom; (B) Induced EF in the experimental phantom.

211

212 2. Experimental set up

213 M Experimental

214

215

216

217

218

219

220

221

As introduced above, the magnetic source is Helmholtz coil. It consists of two loops of 520 mm diameter; each loop consists of 12 contiguous turns made by 16 mm² thick wire (Figure 4). To avoid external electromagnetic disturbances, the Helmholtz coils were placed in a Faraday cage (Lindgren), where the MF exposures for cardiac implants were carried out. The low-frequency exposure system produces homogeneous MFs up to 4000 μ T at 50 Hz and 3900 μ T at 60 Hz, 20 times higher than the limits given in the ICNIRP guidelines. A triaxial MF meter (ESM-100, Maschek Elektronik) was used for monitoring the field strength during tests. Experimental results showed agreement with the analytical solution within $\pm 2\%$ error^[13].

222

223

224

225

226

227

228

229

230

231

232

233

234

235

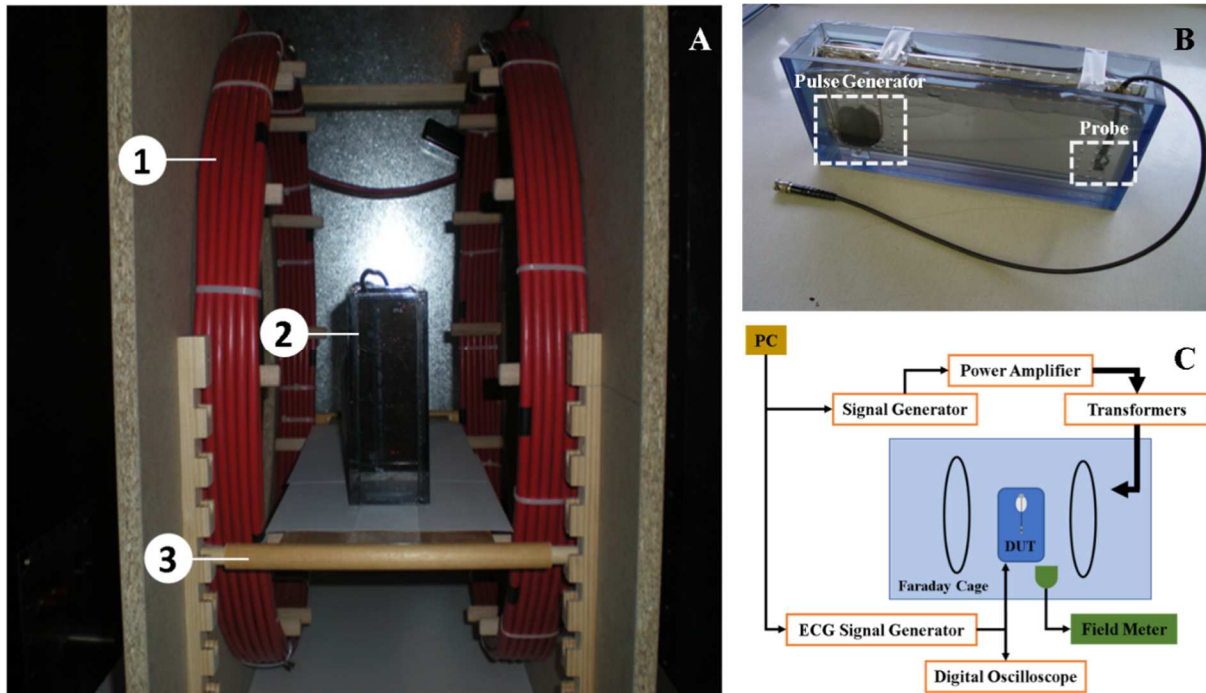
236

237

238

The Helmholtz coils were supplied by a signal generator (HP33120) via a power amplifier (25 VAC, 20 A, 500 VA, 40 Hz-400 kHz). Thanks to a matching system (two transformers), 450 VA was allowed to transmit to the coils. The power unit and the measurement system are all located outside of the Faraday cage, as are a field meter, a digital oscilloscope (TDS3032, Tektronix, Inc.), and a personal computer for data recording. The induction coils and the implanted phantom, as the DUT, are placed on a wooden support in the Faraday cage to avoid distortion of the MF. The cardiac implant is fixed in the experimental phantom tank with a plexiglass support, which ensures reproducible positioning of the ICD and its probe. The distance between the impulse generator of the cardiac implant and the tip electrode is a minimum of 22 cm, based on a 3D scan of an ICD implanted in a human body. The tip-to-ring pair was placed perpendicular to an imaginary line from the impulse generator to the tip-to-ring pair. Based on the numerical study, the field direction was set perpendicular to the induction area, in order to perform the tests in the worst case scenario (frontal exposure). MFs of different strengths and frequencies monitored by the oscilloscope were applied to the cardiac implants for immunity investigation. A coaxial cable was used to inject the simulated heart signal into the cardiac implants. Three types of ECG signal were used: the normal cardiac signal (sinus rhythm (SR), frequency base of 1 Hz), two pathological signals, i.e., ventricular tachycardia (VT, fixed frequency of 2.77 Hz), and ventricular fibrillation (VF, fixed frequency of 3.5 Hz). An amplitude of 5 mV was used for the ECG

239 signals, given that under-sensing is less likely when the SR has a higher amplitude, compared to the
 240 sensing device’s sensitivity, which in turn defines the minimum myocardial voltage required to be
 241 detected as a heart signal.



242
 243 **Figure 4.** MF exposure experimental setting. (A) Inside view of Faraday cage: 1) Helmholtz coils; 2)
 244 DUT; 3) Wooden support. (B) ICD implanted phantom tank (DUT). (C) Schematic diagram of the
 245 implementation

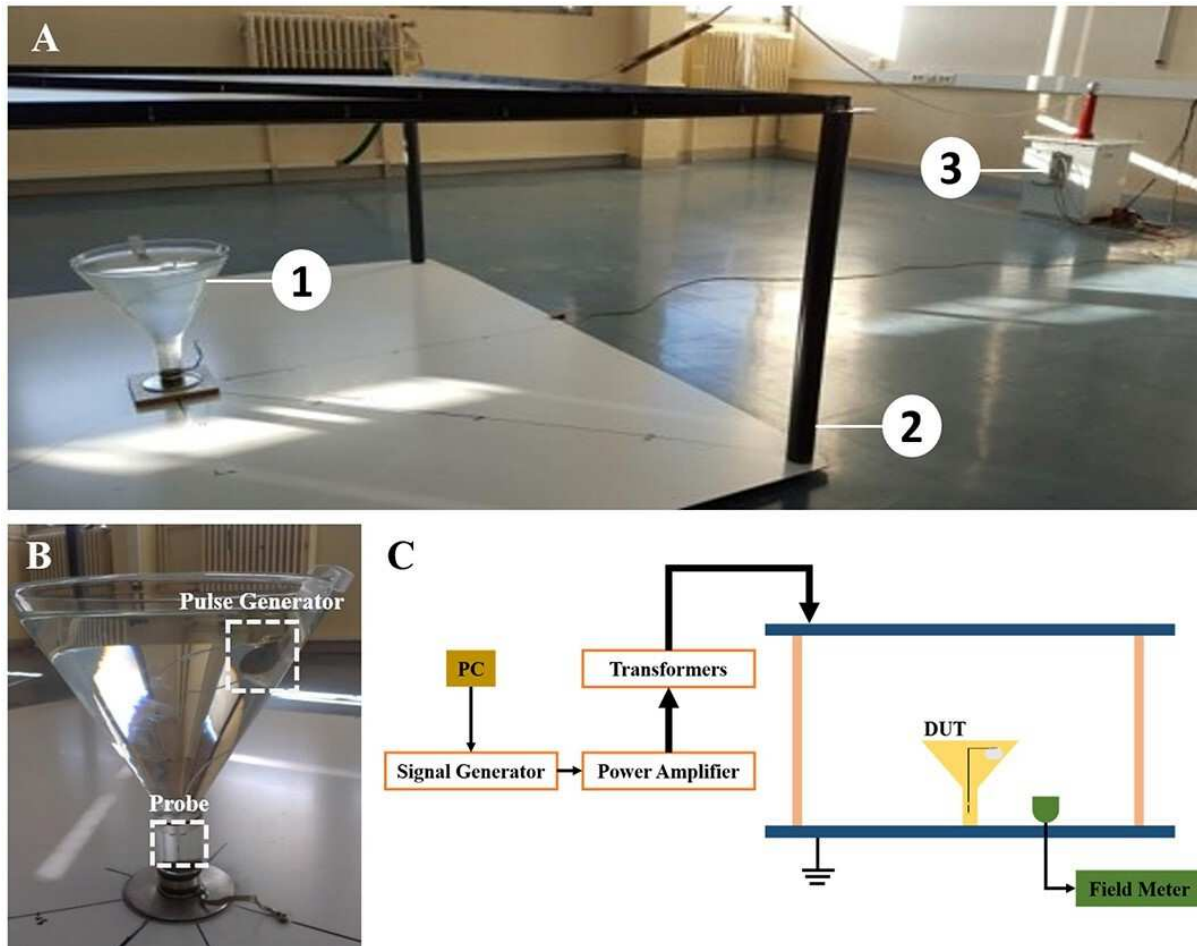
246 Two test protocols were applied in the experimental study. The first followed a provocative study
 247 intending to observe the “false detections,” namely a “dysfunction.” In other words, the goal was to
 248 ascertain whether the cardiac implants interpret the perturbations as arrhythmia. Initially, the magnetic
 249 flux density was set to a minimum value, the frequency of disturbance was fixed (50 or 60 Hz), and an
 250 SR ECG signal was applied to the cardiac implant. A step consisting of 15s pause and 45s exposure was
 251 repeated, with each step increasing by a fixed amount (25 μ T) from 0 μ T to the maximum value. The
 252 second protocol aimed to verify whether the perturbations inhibit the detection of arrhythmia. The initial
 253 factors were the same but the perturbation was continuously applied for the second protocol without
 254 pauses. In addition, instead of a contentiously SR ECG signal, the cardiac implant received the following
 255 signals: VT (15s); SR (45s); VT (15s); SR (45s); VF (15s); SR (45s); VF (15s); SR (45s). A test system
 256 was designed to execute the measurement session automatically, using virtual instrument software HP
 257 VEE under IEEE 488 protocol communication.

258

259 **E Experimental**

260 The experimental EF exposure system was designed to deliver an EF up to 100 kV/m for 50 Hz and 83
 261 kV/m for 60 Hz. The homogeneous EF fields were generated by two aluminum plates (2 m \times 2 m) of
 262 10 mm thickness placed in parallel, 750 mm apart with 4 PVC supports in between. The upper plate was
 263 supplied with a high voltage; the lower plate was grounded. The experimental setup consisted of a signal
 264 generator delivering sinusoidal signals, a power supply, and two transformers that allowed a high voltage
 265 of up to 80 kV to be sent to the conductive plates. A 3D H/E field meter (Maschek ESM-100) was used
 266 to measure the generated field. The room humidity was recorded and maintained at 30–55% during the
 267 experiments, as was temperature, at 19–28 $^{\circ}$ C . The experimental phantom was placed in the center on

268 the lower plate and filled with a solution possessing conductivity of 0.19-0.21 S/m. The conductivity of
 269 the solution was checked by a conductivity meter, HI 99300. The dimensions of the experimental
 270 phantom were the same as those of the numerical study. Plexiglass support allowed the implant housing
 271 to be positioned reproducibly in the container. The end of the probe was guided towards the lower part
 272 (cylindrical part) of the phantom, parallel to the direction of the EF, in order to produce the worst-case
 273 scenario. The phantom was grounded via a connection between its metal bottom and the lower grounded
 274 plate. The setup is shown in Figure 5.



275
 276 **Figure 5.** EF exposure experimental setting. (A) General view: 1) DUT; 2) Aluminum plates and PVC
 277 supports; 3) High voltage transformer. (B) AIMD implanted phantom (DUT). (C) Schematic diagram
 278 of the implementation

279 The cardiac implants were always checked and reset before the tests. Their therapy functions were turned
 280 off. An EF at 1 kV/m was applied to the system at the beginning and increased to 10 kV/m, 3.3 kV/m,
 281 and 1 kV/m, for each trial, until a malfunction occurred. Malfunctions were recorded by the cardiac
 282 implant and retrieved via remote cardiac telemetry after exposure. The malfunctions were tested again
 283 to check their reproducibility. Once identified as reproducible, the EF was decreased to pinpoint the
 284 threshold of the malfunction. We did not apply any cardiac signal to the implant, due to the experimental
 285 difficulty of delivering a cardiac signal without disturbing the induced EF.

286

287 3. Results

288 M Numerical

289 In the numerical study of a bipolar ICD under MF exposures in the vertical position, the induced voltage
 290 on the probe was 0.099 $\mu\text{V}/\mu\text{T}$ for the anatomical model and 0.039 $\mu\text{V}/\mu\text{T}$ for the homogeneous brick
 291 model. The worst-case was found in the frontal position; the induced voltage on the ICD probe was
 292 0.152 $\mu\text{V}/\mu\text{T}$ in the homogeneous brick model.

293 **M Experimental**

294 In the experimental study of MF exposures, four ICDs (three from St. Jude Medical; one from Guidant)
 295 were investigated in a gelatin experimental phantom for nominal sensitivity configurations according to
 296 the established experimental protocol. At the frequency of 50 Hz, no dysfunction was recorded for
 297 exposures up to 2750 μT . At the frequency of 60 Hz, none of the four ICDs showed any malfunction for
 298 exposures up to 2480 μT .

299 **E Numerical**

300 In the study of the anatomical model under EF exposures, the induced voltage between the probe and
 301 the generator in unipolar sensing mode was found to be 223.7 μV ; the induced voltage between the two
 302 electrodes of the probe in bipolar sensing mode was found to be 29.4 μV . We found that the induced
 303 voltage in unipolar sensing mode is 10 times greater in bipolar sensing mode in the case of the right
 304 atrium or right ventricle implantation. The tip-to-ring distance of the lead may have had an influence of
 305 up to 46% on the induced EF. In the bipolar sensing mode, the induced voltage of the right ventricle
 306 implantation was 41% higher than that of the right atrium implantation. The numerical investigation
 307 results yielded an estimated dysfunction threshold of 7.24 kV/m for bipolar sensing mode under the
 308 maximum sensitivity setting. In the simulation of the experimental phantom under 1 kV/m 50 Hz
 309 exposure generated by the exposure system introduced in the previous part, the induced voltage on the
 310 probe of the cardiac implant is 73 μV in the bipolar sensing mode and is 550 μV in the unipolar sensing
 311 mode. An equivalent factor can be defined between the anatomical model and the experimental phantom:
 312 2.45 for the unipolar sensing mode; 2.48 for the bipolar sensing mode.

313 **E Experimental**

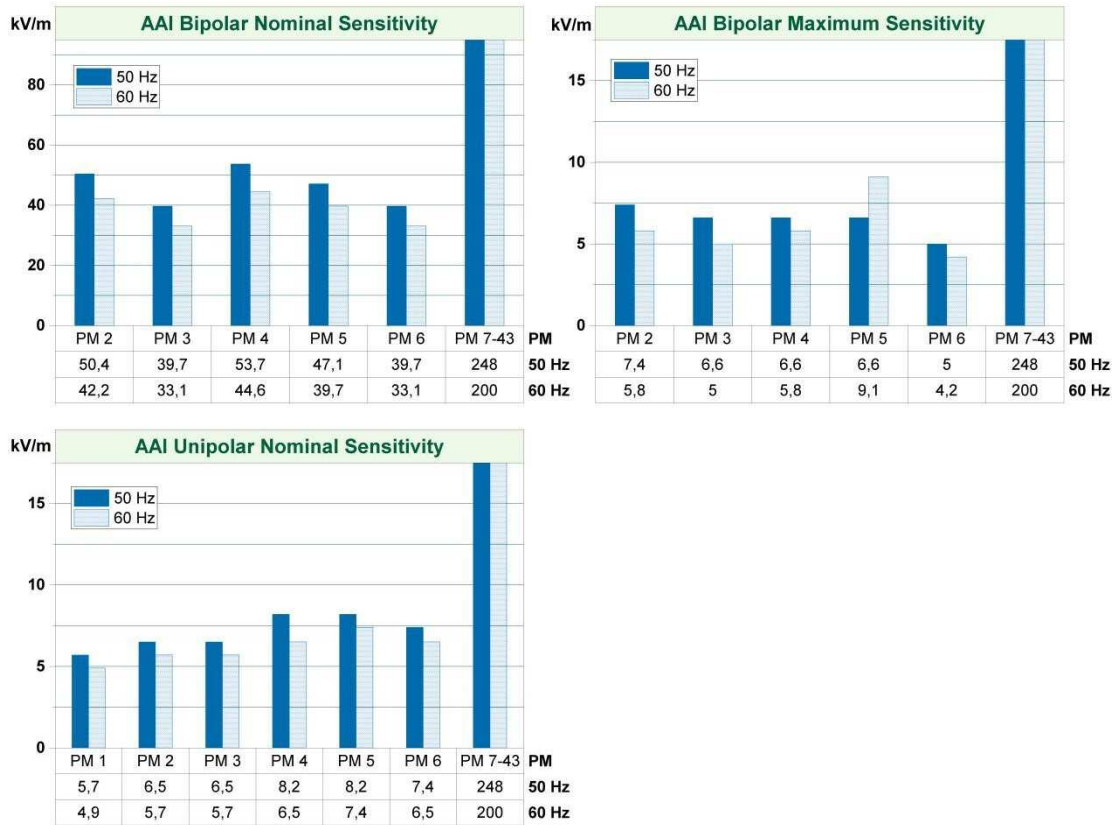
314 Experimental tests were carried out at 50 and 60 Hz to obtain the threshold of dysfunction in the worst-
 315 case scenario. The equivalent factors are applied to the level of EF exposure. 43 PMs and 11 ICDs, from
 316 manufacturers Medtronic, St. Jude Medical, and Vitatron, were tested (see Table 2).

317 **Table 2.** Manufacturer, quantity, models of tested cardiac implants

Type	Manufacturer	Quantity	Model
Implanted Cardiac Defibrillator	Medtronic	10	6
	St. Jude Medical	1	1
Total		11	7
Pacemaker	Medtronic	22	9
	St. Jude Medical	10	8
	Vitatron	11	6
Total		43	28

318

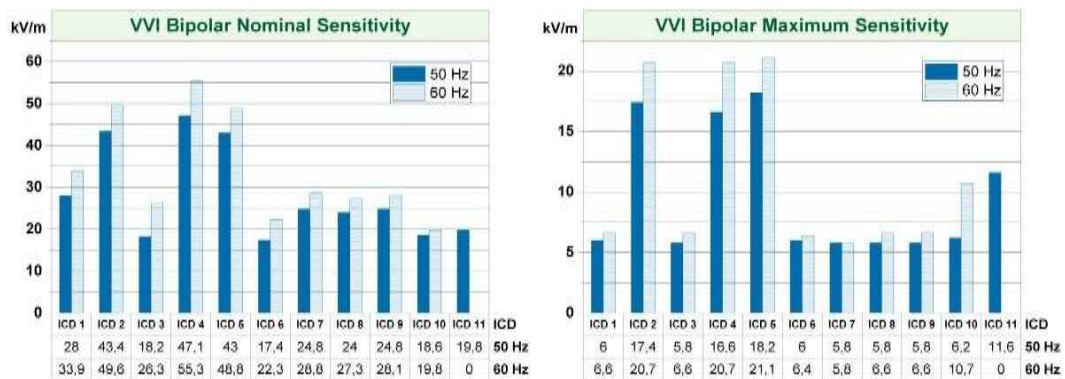
319 No dysfunction was detected on the PMs in ventricular-inhibited (VVI) unipolar sensing mode under
 320 EF exposures up to 245 kV/m at 50 Hz and 198 kV/m at 60 Hz, as well as on the PMs in VVI bipolar
 321 sensing mode up to 248 kV/m at 50 Hz and 200 kV/m at 60 Hz. (Among the 43 PMs, one model worked
 322 only in unipolar sensing mode.) The dysfunction thresholds of the PMs in atrial-inhibited mode (AAI)
 323 with unipolar and bipolar sensing configurations are given in Figure 6.



325

326 **Figure 6.** PM malfunction thresholds under 50 Hz and 60 Hz EF exposure at nominal sensitivity (2
327 mV) and maximum sensitivity (0.2mV)

328 The dysfunction thresholds of ICDs under 50 Hz and 60 Hz EF exposures were investigated for nominal
329 sensitivity (0.6 mV) and maximum sensitivity (0.15 mV for Medtronic ICDs, 0.2 mV for St. Jude ICDs).
330 All 11 ICDs reacted to the EF during the test. The results are given in Figure 7.



331

332 **Figure 7.** ICD malfunction thresholds under 50Hz and 60 Hz EF exposure at nominal sensitivity
333 (0.6mV) and maximum sensitivity (0.15 / 0.2mV)

334

335 Discussion

336 In the study of MF exposure, the induced voltage on the probe of a bipolar ICD under exposure was
337 found to be $0.152 \mu\text{V}/\mu\text{T}$ for the worst case, which provided a reference value for future experimental
338 studies. In the *in vitro* study, none of the four ICDs were susceptible to EMI in very high MFs (2.75 mT
339 at 50 Hz, 2.48 mT at 60 Hz). This supports the premise that ICDs are safe in terms of MF dysfunction.
340 Among the reasons for the good ICD performance in our tests is the fact that the bipolar sensing mode
341 of the electrodes is significantly improved compared to unipolar sensing (Trigano, 2005). Moreover, the
342 input/output filters of the tested ICDs provide excellent immunity to low-frequency MFs. ICDs did not
343 misinterpret noise from EMI as VT or VF, nor did they deliver inappropriate defibrillation. MF
344 intensities applied in this study are rare or even altogether absent in the industrial workplace. These
345 settings and protocols provide useful tools for researchers and clinicians, allowing for the testing of
346 ICDs in a realistic way and also ensuring repeatability of results. They could also be useful in the design
347 of risk assessments for ICD wearers returning to their jobs in EM professional environments after having
348 devices implanted. Our team also carried out a study on PMs under MF exposures in the 2000s. However,
349 with the rapid development of AIMD technology, the latest models of PMs should be taken into
350 consideration. Thus, future investigations of PMs under occupational exposures could be conducted with
351 the new setup proposed in this study.

352 In the EF exposure component of this work, equivalent factors between the models were found in the
353 numerical study. Between the anatomical model and the experimental phantom, an equivalent factor of
354 2.45 was found for the unipolar sensing mode; 2.48 was found for the bipolar sensing mode. The
355 equivalent factor enables the conversion of study from the anatomical model to the experimental model.
356 The results of induced voltage provide reference values for future experimental measurements. Our *in*
357 *vitro* experimental study tested 54 cardiac implants, including 7 different types over 11 ICDs and 28
358 different types of 43 PMs, in the presence of EFs up to 248 kV/m at 50 Hz and 200 kV/m at 60 Hz. The
359 results pinpoint the field levels that lead to potential risks of EMI-caused dysfunctions, which may cause
360 clinically significant events. Results were obtained for the very disadvantaged scenarios, the worst case
361 of the given conditions or very close to it. We observed rare cases where EMI caused PMs and ICDs to
362 switch into noise mode, which means that they continued to deliver the standard heartbeat. No risk of
363 false treatment under public exposure was observed. When PMs and ICDs are configured with
364 maximum bipolar sensitivity or nominal unipolar sensitivity, occupational exposure may present some
365 risks. According to our results, there is no risk for implants configured in bipolar mode with nominal
366 sensitivity in working environments (conforms to EU directives).

367

368 CONCLUSION

369 In this work, theoretical and experimental studies of cardiac implant wearers exposed to extremely low
370 frequency (50/60 Hz) EF and MF were carried out. We presented a protocol and a setup dedicated to
371 investigating the operational integrity of cardiac implants under low frequency homogeneous
372 electromagnetic exposures. An analysis of the EFs induced in the human body during exposure aimed
373 at determining the induction in each organ of a virtual anatomical model. Likewise, the numerical
374 calculation of the voltage induced at the tip of the probe was performed in the virtual human model
375 containing a cardiac implant. The calculations are based on a finite integral method element model using
376 CST® software.

377 Experimentally, *in vitro* tests were carried out in very high MF/EF levels (up to 4 mT for MF; up to 248
378 kV/m for EF). We note from our results that a significant risk of dysfunction occurred on carriers of
379 PMs in the unipolar mode under EF exposure. Our results suggest that, in almost all cases, workplaces
380 exposing employees to a 50 Hz MF or EF are not likely to cause electromagnetic interference, given a
381 setting with nominal sensitivity; in contrast, a maximum sensitivity configuration may lead to a risk of
382 interference. A case-by-case risk assessment study is required. Conducting a thorough and detailed study

383 of each situation, accounting for patients' shape features as well as the implant configuration, must be
384 considered.

385 Studying the treatment performance of AIMD under EMF exposures provides the complementary
386 characterization of AIMD behaviors. Real-time measurements of the induced voltage on the cardiac
387 implant probe under exposure allowed us to conduct further observations of the behaviors of cardiac
388 implants and to draw comparisons with the theoretical results.

389

390 **ABBREVIATIONS**

391 AIMD: Active implantable medical devices; EMF: Electromagnetic field; EF: Electric field; MF:
392 Magnetic field; PM: Pacemaker; ICD: Implantable cardioverter defibrillator; Hz: Hertz; A/m: Amperes
393 per meter; kV/m: Kilovolt/meter; $\mu(m)T$: Micro (Milli) Tesla; S/m: Siemens per meter; DUT: Device
394 under test; SR: Sinus rhythm; VT: Ventricular tachycardia; VF: Ventricular fibrillation; VVI:
395 Ventricular-inhibited mode. AAI: Atrial-inhibited mode.

396

397 **Funding**

398 This project was supported by Réseau de Transport d'Électricité and Électricité de France.

399

400 **Declaration of interest**

401 The authors declare no competing interests.

402

403 **Ethical Approval**

404 Not required.

405

406 **References**

407 [1] Virani SS, Alonso A, Aparicio HJ, Benjamin EJ, Bittencourt MS, Callaway CW, et al., 2021. Heart
408 Disease and Stroke Statistics—2021 Update: A Report from the American Heart Association *Circulation*.
409 2021;143:e254–e743.

410 [2] Timmis, A., Townsend, N., Gale, C., Grobbee, R., Maniadakis, N., Flather, M., et al., 2017. European
411 Society of Cardiology: Cardiovascular Disease Statistics 2017. *European Heart Journal*, 39(7), pp.508–
412 579.

413 [3] Raatikainen, M., Arnar, D., Merkely, B., Nielsen, J., Hindricks, G., Heidbuchel, H. and Camm, J.,
414 2017. A Decade of Information on the Use of Cardiac Implantable Electronic Devices and Interventional
415 Electrophysiological Procedures in the European Society of Cardiology Countries: 2017 Report from
416 the European Heart Rhythm Association. *EP Europace*, 19(suppl_2), pp.ii1–ii90.

417 [4] Mattei, E., Calcagnini, G., Censi, F., Pinto, I., Bogi, A. and Falsaperla, R., 2019. Workers with Active
418 Implantable Medical Devices Exposed to EMF: In Vitro Test for the Risk Assessment. *Environments*,
419 6(11), p.119.

- 420 [5] Korpinen, L., Kuisti, H., Elovaara, J. and Virtanen, V., 2012. Cardiac Pacemakers in Electric and
421 Magnetic Fields of 400-kV Power Lines. *Pacing and Clinical Electrophysiology*, 35(4), pp.422–430.
- 422 [6] Korpinen, L., Kuisti, H., Elovaara, J. and Virtanen, V., 2013. Implantable Cardioverter Defibrillators
423 in Electric and Magnetic Fields of 400 kV Power Lines. *Pacing and Clinical Electrophysiology*, 37(3),
424 pp.297–303.
- 425 [7] Korpinen, L., Kuisti, H., Tarao, H., Elovaara, J. and Virtanen, V., 2014. Implantable Cardioverter
426 Defibrillators in Magnetic Fields of a 400kV Substation. *Progress In Electromagnetics Research M*, 40,
427 pp.205–213.
- 428 [8] Tiikkaja, M., Aro, A., Alanko, T., Lindholm, H., Sistonen, H., Hartikainen, J., Toivonen, L.,
429 Juutilainen, J. and Hietanen, M., 2013. Testing of Common Electromagnetic Environments for Risk of
430 Interference with Cardiac Pacemaker Function. *Safety and Health at Work*, 4(3), pp.156–159.
- 431 [9] Parakh, N., Parashar, N. and Sinha, M., 2018. Safety of Magnetic Resonance Imaging in Patients
432 with Cardiac Devices. *Journal of the Practice of Cardiovascular Sciences*, 4(1), p.37.
- 433 [10] Stunder, D., Seckler, T., Joosten, S., Zink, M., Driessen, S., Kraus, T., Marx, N. and Napp, A., 2017.
434 In Vivo Study of Electromagnetic Interference with Pacemakers Caused by Everyday Electric and
435 Magnetic Fields. *Circulation*, 135(9), pp.907–909.
- 436 [11] Health Physics, 2010. Guidelines for Limiting Exposure to Time-varying Electric and Magnetic
437 Fields (1 Hz TO 100 kHz). 99(6), pp.818–836.
- 438 [12] European Committee for Electrotechnical Standardization (CENELEC) 2010. Procedure for the
439 Assessment of the Exposure to Electromagnetic Fields of Workers bearing Active Implantable Medical
440 Devices (Brussels: European Committee for Electrotechnical Standardization)
- 441 [13] Katrib, J., Nadi, M., Kourtiche, D., Magne, I., Schmitt, P., Souques, M. and Roth, P., 2013. In vitro
442 assessment of the immunity of implantable cardioverter-defibrillators to magnetic fields of 50/60 Hz.
443 *Physiological Measurement*, 34(10), pp.1281–1292.
- 444 [14] Gerçek, C., Kourtiche, D., Nadi, M., Magne, I., Schmitt, P., Roth, P. and Souques, M., 2020.
445 Phantom Model Testing of Active Implantable Cardiac Devices at 50/60 Hz Electric Field.
446 *Bioelectromagnetics*, 41(2), pp.136–147.
- 447 [15] Gerçek, C., Kourtiche, D., Nadi, M., Magne, I., Schmitt, P., Souques, M. and Roth, P., 2017. An In
448 Vitro Cost-Effective Test Bench for Active Cardiac Implants, Reproducing Human Exposure to Electric
449 Fields 50 Hz. *International Journal on Smart Sensing and Intelligent Systems*, 10(1), pp.1–17.
- 450 [16] Gerçek, C., Kourtiche, D., Nadi, M., Magne, I., Schmitt, P. and Souques, M., 2017. Computation
451 of Pacemakers Immunity to 50 Hz Electric Field: Induced Voltages 10 Times Greater in Unipolar Than
452 in Bipolar Detection Mode. *Bioengineering*, 4(4), p.19.
- 453 [17] IEC 62226-2-1. Exposure to electric or magnetic fields in the low and intermediate frequency
454 range—Methods for calculating the current density and internal electric field induced in the human body
455 —Part 2-1: Exposure to magnetic fields—2D models.
- 456 [18] IEC 62226-3-1. Exposure to electric or magnetic fields in the low and intermediate frequency
457 range—Methods for calculating the current density and internal electric field induced in the human
458 body—Part 3-1: Exposure to electric fields—Analytical and 2D numerical models. Ed. 2016.

- 459 [19] A. Christ et al., 2010. The Virtual Family—Development of Surface-Based Anatomical Models of
460 Two Adults and Two Children for Dosimetric Simulations, *Physics in Medicine and Biology*, vol. 55,
461 n°. 2, p23–38.
- 462 [20] Hasgall PA, Di Gennaro F, Baumgartner C, Neufeld E, Lloyd B, Gosselin MC, Payne D,
463 Klingenböck A, Kuster N, 2014. IT'IS Database for Thermal and Electromagnetic Parameters of
464 Biological Tissues, Version 2.5, Aout 07, DOI: 10.13099/ViP-Database-V2.5
- 465 [21] Marchal, C., Nadi, M., Tosser, A., Roussey, C. and Gaulard, M., 1989. Dielectric Properties of
466 Gelatine Phantoms used for Simulations of Biological Tissues between 10 and 50 MHz. *International*
467 *Journal of Hyperthermia*, 5(6), pp.725–732.
- 468 [22] Gustrau, F., Bahr, A., Goltz, S. and Eggert, S., 2002. Active Medical Implants and Occupational
469 Safety—Measurement and Numerical Calculation of Interference Voltage. *Biomedizinische*
470 *Technik/Biomedical Engineering*, 47(s1b), pp.656–659.